Modular Response in Free Quantum Fields: A KMS/FDT Theorem and Conditional Extensions

[Authors][1]

[1] *[Institutions]*

(Dated:)

Part I (Theoremic core, free/Gaussian Hadamard QFT). We prove that, for small causal diamonds (CHM) in locally Hadamard states and within a safe window $\epsilon_{\rm UV} \ll \ell \ll \min\{L_{\rm curv}, \lambda_{\rm mfp}, m_i^{-1}\}$, the MI/moment-kill projector isolates a finite ℓ^4 modular response with coefficient equal to its flat-space value; the projected KMS/FDT susceptibility is positive; and coarse-graining over the wedge family produces the universal weak-field prefactor $5/12 = (4/3)\times(5/16)$. The fractional KMS defect between CHM diamonds and half-spaces scales as $\mathcal{O}((\ell/L_{\rm curv})^2) + \mathcal{O}((\ell H)^2)$. The QFT sensitivity is $\beta = 2\pi C_T I_{00} = 0.02086 \pm 0.00105$ (conservative 5% shared systematics from four independent routes). A scheme-invariant background relation *suggests* $\Omega_\Lambda = \beta\, f\, c_{\rm geo}$ *conditional* on our coarse-graining and analyticity assumptions.

Part II (Conditional extensions). We separate *definition* (flat-space ε from modular response) from *mapping*. Rather than impose the standard EFT-of-DE α-basis, we adopt a quasi-static closure that keeps operational distances GR-like (no additional lensing coupling $\Sigma \simeq 1$) while modifying growth via $\mu(\varepsilon) = 1/(1 + \frac{5}{12}\varepsilon)$. KMS/FDT positivity motivates an entropy-driven law $d\varepsilon/d\ln a \geq 0$ with a *conditional* background budget $\int \varepsilon\, d\ln a = \Omega_\Lambda$. We introduce a covariant environment envelope $F_g(\chi_g) = [1 + (\chi_g/\chi_\star)^q]^{-1}$ with $\chi_g \equiv \ell^2\sqrt{C_{abcd}C^{abcd}}$, calibrated by Solar-System bounds. Cosmological illustrations (S_8 band and H_0 bounds) are **toy/illustrative** and propagate the $\pm 5\%$ β uncertainty; *observed lensing amplitudes still reflect the altered growth.*

Part III (Exploratory). We provide a compact *thermodynamic interpretation* of the projected modular response: a Clausius-like identity holds at working order in the MI/moment-kill channel, and the FRW budget may be viewed as a *coarse-grained* Clausius normalization *conditional* on our KMS→FRW hypotheses. We clarify the relation to the Casini–Galante–Myers critique of Jacobson; our MI projection targets the ℓ^4 response and deliberately avoids marginal $\Delta = d/2$ logarithms, with $\ell^4 \log \ell$ taken as a falsifier.

What is new. (i) Completed proofs in the Gaussian/Hadamard sector; (ii) a **conditional, coarse-grained** KMS→FRW averaging statement with explicit error budget; (iii) **Assumptions C and D stated with rationale** (relative entropy ↔ canonical energy in the projected diamond; uniqueness of M^2 at working order), with proofs deferred; (iv) semi-analytic quantification of the safe-window volume fraction $f_V(\ell_{\rm min})$; (v) a symmetry-constrained F_g envelope; (vi) uncertainty propagation of β into S_8 and H_0 *illustrations*; (vii) an exploratory thermodynamic reinterpretation (Part III) and refined treatment of the CGM critique.

READER'S MAP: PART I (THEOREM) VS. PART II (CONDITIONAL) VS. PART III (EXPLORATORY)

Part I (Secs. I–IV, Apps. XV–XVIII): proven results for free/Gaussian Hadamard fields at working order.
Part II (Secs. V–XXII, Apps. XIX–XX, XXI): conditional extensions, Assumptions C & D (stated), safe-window fraction, KMS→FRW link, symmetry envelope, entropic sketch, and toy/illustrative numerics with propagated uncertainties.
Part III (Sec. XIII): exploratory thermodynamic interpretation (Clausius form in the projected channel; conditional FRW budget) and relation to CGM's critique of Jacobson.

I. SCOPE, WORKING ORDER, AND SAFE-WINDOW QUANTIFICATION (PART I)

a. Working order and state class. We work to $\mathcal{O}(\ell^4)$ in the MI/moment-kill projector channel, treating curvature/contact terms as $\mathcal{O}(\ell^6)$. States are locally Hadamard.

b. KMS applicability (CHM diamonds). Exact BW KMS holds for half-spaces; CHM diamonds inherit it with fractional defect $\mathcal{O}((\ell/L_{\rm curv})^2) + \mathcal{O}((\ell H)^2)$ (App. XVIII).

c. Safe-window volume fraction. Define a conservative admissible scale

$$\ell_{\rm max}(x) \equiv \zeta\ \min\Big\{L_{\rm curv}(x),\ \lambda_{\rm mfp}(x),\ m_i^{-1}(x)\Big\}, \qquad \zeta = 0.1. \tag{1}$$

Using Press–Schechter/Sheth–Tormen mass functions and NFW curvature proxies $L_{\rm curv}^{-2} \sim (R_{abcd}R^{abcd})^{1/2}$ with substructure excision parameter ξ, we estimate the comoving volume fraction $f_V(\ell_{\rm min}) = {\rm Vol}\{x : \ell_{\rm max}(x) > \ell_{\rm min}\}/{\rm Vol}_{\rm tot}$. A semi-analytic survey (App. XIX) shows voids dominate f_V, while dense cores lack a window; representative values at $z\sim 0$ for $\ell_{\rm min} \in [1, 100]$ pc are $f_V \sim 0.6{-}0.95$ for $\xi \in [0.2, 0.5]$. This enters only as a domain-of-validity indicator.

d. Spectrum caveat. The admissible window $\epsilon_{\rm UV} \ll \ell \ll \min\{L_{\rm curv}, \lambda_{\rm mfp}, m_i^{-1}\}$ is understood to apply to sectors that contribute at working order. Massive sectors with $\ell \gg m_i^{-1}$ are exponentially suppressed and, after MI/moment–kill subtraction, do not re-introduce lower moments or $\ell^4 \log \ell$ terms. Thus the ℓ^4 coefficient is dominated by massless/light fields while heavy fields decouple in this channel.

e. Angle invariance as a null test. The continuous-angle product $\mathcal{C}_\Omega = f(\theta)\, c_{\rm geo}(\theta)$ is analytic and θ-independent; residuals are shown as a null check, not a precision claim.

II. A2–KMS THEOREM (GAUSSIAN/HADAMARD SECTOR)

Theorem 1 (Projected modular response and positivity)**.** *Let $\mathcal{Q}$ be a free (Gaussian) QFT on a globally hyperbolic spacetime and ρ a locally Hadamard state. For a causal diamond of radius ℓ with $\ell \ll L_{\rm curv}$ and the MI/moment-kill projector that cancels r^0 and r^2 moments, the MI-subtracted modular response obeys*

$$\delta\langle K_{\rm sub}\rangle = (2\pi C_T I_{00})\, \ell^4\, \delta\varepsilon + \mathcal{O}(\ell^6), \tag{2}$$

with coefficient equal to the flat-space value. The retarded susceptibility χ_{QK} in the projected channel is positive (FDT), and wedge averaging yields the universal weak-field prefactor $5/12$. The fractional deviation from BW KMS is $\mathcal{O}((\ell/L_{\rm curv})^2) + \mathcal{O}((\ell H)^2)$.

Corollary 1 (Conditional background statement)**.** *Under the coarse-graining and analyticity assumptions of Sec. VI, the FRW zero mode* suggests *the scheme-invariant relation $\Omega_\Lambda = \beta\, f\, c_{\rm geo}$ with $\beta = 2\pi C_T I_{00}$. We treat this as a conditional statement rather than a theorem.*

III. QFT INPUT: $\beta = 2\pi C_T I_{00}$ AND ERROR BUDGET

We evaluate β via four independent routes: (a) real-space CHM; (b) spectral/Bessel; (c) Euclidean time-slicing; (d) replica finite-difference. The spread is $\lesssim 1\%$. We adopt a conservative

$$\beta = 0.02086 \pm 0.00105 \quad (5\% \text{ shared systematics}). \tag{3}$$

Angle invariance is used as a null residual test.

Here C_T denotes the flat-space stress-tensor two-point normalization, e.g. $\langle T_{ab}(x)\, T_{cd}(0)\rangle = C_T\, \mathcal{I}_{abcd}(x)/|x|^{2d}$ in d dimensions (see Osborn–Petkou).

Benchmark (convention). For a free, massless real scalar in $d = 4$ and our normalization, $C_T = 1/(120\pi^2)$, which yields $\beta \simeq 0.02086$ via Eq. (4).

Reproducibility. For the MI/moment-kill weights used in our numerics (App. XV), the projected integral evaluates to

$$I_{00} = 3.932017 \quad (\text{dimensionless}),$$

so with $C_T = 1/(120\pi^2)$ one obtains $\beta = 2\pi C_T I_{00} = 0.02086$ as quoted. The helper script `beta_methods_v2.py` prints this I_{00} value.

IV. WEAK-FIELD PREFACTOR 5/12

The isotropic BW channel gives $\langle T_{kk}\rangle = (1+w)\rho$ with UV $w = 1/3 \Rightarrow 4/3$. Averaging over CHM segments yields $5/16$, so $5/12 = (4/3) \times (5/16)$. Details in App. XVII.

V. DEFINITION VS. MAPPING (PART II; CONDITIONAL)

a. Definition (flat-space QFT).

$$\delta\langle K_{\rm sub}(\ell)\rangle = \underbrace{(2\pi C_T I_{00})}_{\beta}\, \ell^4\, \delta\varepsilon(x) + \mathcal{O}(\ell^6). \tag{4}$$

b. Mapping (constitutive; beyond the α-basis). We *do not* impose the linear EFT-of-DE α-parameter mapping at working order. Instead, we adopt a quasi-static closure that keeps operational distances GR-like while modifying growth:

$$\nabla^2\Phi \;=\; 4\pi G a^2 \rho_m\, \mu(\varepsilon)\, F_g(\chi_g), \qquad \mu(\varepsilon) = \frac{1}{1+\frac{5}{12}\varepsilon}, \tag{5a}$$

$$\nabla^2 \frac{\Phi+\Psi}{2} \;=\; 4\pi G a^2 \rho_m, \qquad (\Sigma \simeq 1). \tag{5b}$$

Matter obeys the standard continuity and Euler equations. This closure preserves the Bianchi identity at working order provided F_g is a scalar built from local geometry (Sec. IX); a full action-level derivation is future work (Limitations). *Remark on lensing amplitude.* $\Sigma \simeq 1$ denotes no additional lensing coupling; the observed lensing signal still changes through the altered growth $D(a)$.

c. EFT stub (derivation of $\mu(\varepsilon)$). At quasi-static, sub-horizon scales, a background variation $\delta \ln M^2 = \beta\,\delta\varepsilon$ rescales the Poisson coupling as $G \to G_{\rm eff} = G/(1+\Delta)$ with Δ fixed by the universal weak-field bookkeeping. In the isotropic BW channel the contraction 4/3 and the segment ratio 5/16 (Sec. IV) give $\Delta = \frac{5}{12}\varepsilon$, hence

$$\mu(\varepsilon) = \frac{G_{\rm eff}}{G} = \frac{1}{1+\frac{5}{12}\varepsilon}\,, \tag{6}$$

consistent with Eqs. (5).

d. Trial action (outlook). A possible action-level route consistent with our closure is to consider an effective term that modulates M^2 via the modular response,

$$S_{\rm trial} = \int d^4x\,\sqrt{-g}\left[\frac{M^2}{2}R + \lambda\,(\delta \ln M^2)\,\mathcal{K}[g;\ell] + \cdots\right],$$

where $\mathcal{K}$ is a local covariant scalar capturing the projected channel at working order and λ a running coefficient. While only illustrative, this shows how $\delta \ln M^2 = \beta\,\delta\varepsilon$ could arise from an action (cf. [6, 8]).

Weak-field acceleration (toy/conditional). Using the universal 5/12 prefactor and the *conditional* background relation $\Omega_\Lambda = \beta f c_{\rm geo}$, the weak-field normalization implies a MOND-like acceleration scale

$$a_0 = \frac{5}{12}\,\Omega_\Lambda^2\, c\, H_0, \tag{7}$$

reported as an *illustrative* consequence pending validation of the interacting extensions and the KMS→FRW link (Sec. VI). Pipeline values propagate the ±5% uncertainty in β.

This is a **constitutive closure**, not a derived macroscopic law; it is falsified by log-ℓ residuals, $|d_L^{\rm GW}/d_L^{\rm EM} - 1| > 5\times10^{-3}$, or Ω_Λ inconsistent with $\beta f c_{\rm geo}$.

VI. COVARIANT KMS → FRW LINK AND ERROR CONTROL

Let s denote modular time with $\beta_{\rm KMS} = 2\pi/\kappa$ locally, where κ is the local boost surface gravity so that the approximate conformal Killing field ξ^a satisfies $\xi^a\nabla_a = \kappa\,\partial_s$. Averaging the retarded kernel over a comoving congruence of diamonds and reparametrizing $s \mapsto \ln a$ induces the FRW background factor $f\,c_{\rm geo}$; diffeomorphism covariance is preserved because the averaging functional depends only on local curvature scalars and the diamond foliation. The total fractional defect in the kernel obeys

$$\frac{\delta\chi}{\chi_{\rm BW}} = \mathcal{O}\Big((\ell/L_{\rm curv})^2\Big) + \mathcal{O}\big((\ell H)^2\big), \tag{8}$$

which is negligible for $\ell \sim 10\,$pc, $L_{\rm curv} \sim 10\,$Mpc, $H^{-1} \sim 4\,$Gpc.

Proposition 1 (FRW budget identity (conditional; analyticity hypothesis))**.** *Assume: (H1) locality and rapid decay of the spatially averaged, projected retarded kernel so that its reparametrization defines a distribution in* $\ln a$*; (H2) adiabatic evolution through matter domination so that* $J(a) = ds/d\ln a \propto H(a)^{-1}$ *varies slowly; (H3) preservation of*

KMS analyticity of the averaged kernel under the reparametrization $s \to \ln a$; and (H4) negligible CHM vs. half-space deviation at working order (App. XVIII). Then

$$\left\langle \int \chi_{QK}^{\mathrm{proj}}(a,a')\, d^3x \right\rangle = \beta\, f\, c_{\mathrm{geo}}\, \delta(\ln a - \ln a') + \dots$$

and integrating the entropy-driven evolution $d\varepsilon/d\ln a = \sigma(a) I(a) \geq 0$ yields the coarse-grained identity

$$\int_{a_i}^{1} \varepsilon(a)\, d\ln a \;=\; \Omega_\Lambda \;=\; \beta\, f\, c_{\mathrm{geo}}, \tag{9}$$

used as a normalization under (H1)–(H4).

Operational diagnostic. The routine `referee_pipeline.py` reports a scalar residual $R_{\mathrm{nonloc}} \equiv \sum_{i\neq 0} \left|\bar{\chi}^{\mathrm{proj}}(\Delta_i)\right| \Delta(\ln a)_i$ outside the contact bin; a statistically significant non-zero R_{nonloc} falsifies (H1).

Proof sketch. Average the projected KMS kernel over the diamond foliation; reparametrize modular time s to $\ln a$ with Jacobian $J(a) \propto H^{-1}$. Under (H1)–(H3) the averaged kernel remains a positive KMS/FDT object and collapses to a contact term in $\ln a$ at working order, with angle factor $f c_{\mathrm{geo}}$. (H4) bounds the half-space/diamond deviation. Integrating the positive evolution law then fixes the budget (9). □

Geometric origin. The factor $f\, c_{\mathrm{geo}}$ depends only on the wedge-family foliation and unit–solid–angle normalization; it is geometric and foliation-based, not a fit parameter (Appendix XVI).

Analyticity caveat. The reparametrization $s \to \ln a$ is conjectured to preserve KMS analyticity of the *averaged* retarded kernel; a proof likely requires a spectral/microlocal argument (cf. modular-Hamiltonian spectral decompositions in [12] and the curved-spacetime microlocal analysis of [10]). A failure would manifest as non-local or non-analytic kernels in $\ln a$, which our simulations can detect via residuals in the projected susceptibility. We therefore treat the KMS→FRW link as a controlled conjecture with the error budget in Eq. (8).

a. Thermodynamic analogy (pointer). The entanglement first law suggests a Clausius-like analogy (Sec. XIII), *conditional* on (H1)–(H4), with MI projection avoiding CGM's marginality issues (App. XX).

VII. ASSUMPTIONS FOR INTERACTING EXTENSIONS AT WORKING ORDER (PART II; STATED AND TEST CRITERIA)

A. Assumption C (stated; test criteria): Relative entropy ↔ canonical energy in the projected diamond

Statement. For a local algebra $\mathcal{A}(B_\ell)$ of an interacting Hadamard QFT obeying the microlocal spectrum condition and time-slice axiom, the MI/moment-kill projected second variation of Araki relative entropy equals the canonical-energy quadratic form of the projected stress tensor, up to $\mathcal{O}(\ell^6)$ remainders, with a positive-definite projected kernel $\chi_{QK}^{\mathrm{proj}}$.

Rationale (sketch). (i) The second variation is the Bogoliubov–Kubo–Mori metric. (ii) The MI/moment-kill projector cancels local counterterms to $\mathcal{O}(\ell^4)$ (App. XV), conjectured to persist in interacting Hadamard QFTs (App. XX). (iii) Diffeomorphism Ward identities match the BKM quadratic form to canonical energy in the CHM channel. (iv) Positivity follows from KMS/BKM positivity in the projected channel. A complete microlocal proof is left to future work.

a. Operational tests (pass/fail).

- **Positivity test (substrates):** The projected, integrated retarded kernel $\int \chi_{QK}^{\mathrm{proj}}\, d^4x\, d^4x'$ is nonnegative in Gaussian chains (exact) and HQTFIM (numerical tolerance) (checked with `hqtfim_capacity_probe.py`, `gaussian_capacity_probe.py`).
- **No-$\ell^4 \log \ell$ falsifier:** The MI/moment-kill channel exhibits no $\ell^4 \log \ell$ term. *Fail* if a protected-operator contribution produces an $\ell^4 \log \ell$ trend.
- **Plateau stability:** Varying MI windows leaves the residual plateau $\sim \mathcal{O}(\ell^6)$ (verifiable with `beta_methods_v2.py`). *Fail* if residuals scale as ℓ^4 after subtraction.
- **BKM positivity (finite truncations):** In truncated QFTs, the BKM quadratic form for δK_{sub} is positive definite (tested with `gaussian_capacity_probe.py`). *Fail* if negative eigenmodes persist under refinement.

B. Assumption D (stated; test criteria): Uniqueness of the M^2 coupling at working order

Statement. In the $c_T=1$, $\alpha_B=0$ EFT corner linearized about FRW, with isotropy, parity, and time-reversal, the only background scalar coupling that survives the MI/moment-kill projection at $\mathcal{O}(\ell^4)$ and modifies the weak-field growth sector while keeping distances GR-like is $\delta \ln M^2$; other diffeomorphism-invariant local scalars are projected out, forbidden by sector constraints, or curvature-suppressed by $\mathcal{O}((\ell/L_{\rm curv})^2)$.

Rationale (sketch). Consider the most general local covariant functional at the required engineering dimension:

$$\delta\mathcal{L} = \sqrt{-g}\left[a\,R + b\,R_{ab}R^{ab} + c\,\nabla^2 R + d\,\delta\ln M^2\,R + e\,\delta g^{00} + f\,K\,\delta g^{00} + \cdots\right], \tag{10}$$

where "$\cdots$" denote terms of higher engineering dimension (e.g., $\nabla^4 R$, R^4) or parity-odd contributions, excluded by the MI/moment-kill projector and EFT symmetry constraints at $\mathcal{O}(\ell^4)$. Imposing $c_T = 1$ excludes tensor-speed shifts; $\alpha_B = 0$ removes braiding operators; isotropy/time-reversal exclude vector/tensor backgrounds. The projector cancels r^0, r^2 and total derivatives like $\nabla^2 R$; R and $R_{ab}R^{ab}$ are curvature-suppressed. Thus $\delta\ln M^2$ is the unique working-order scalar affecting growth without changing distances.

a. Operational tests (pass/fail).

- **GR-like distances:** EM/GW luminosity distances agree at working order, $|d_L^{\rm GW}/d_L^{\rm EM} - 1| \lesssim 5\times10^{-3}$. *Fail* if a lensing coupling $\Sigma \neq 1$ is required.
- **Growth-only modification:** Large-scale growth follows $\mu(\varepsilon)$ with $\Sigma \simeq 1$ and standard continuity/Euler equations. *Fail* if background α_M must vary appreciably to reproduce $\mu \neq 1$.
- **Solar-System compliance:** Envelope $F_g(\chi_g)$ suppresses deviations: $F_g(\chi_\odot) \ll 10^{-5}$. *Fail* if planetary bounds are violated.
- **Falsifier link:** Any of the falsifiers in Sec. XII triggers failure of Assumption D.

VIII. ENTROPY-DRIVEN $\varepsilon(a)$ AND GROWTH (CONDITIONAL)

a. KMS/FDT positivity. Let $\hat{Q}$ be the boost-energy flux and $\chi_{QK}^{\rm proj}$ the retarded kernel in the projected channel. Then

$$\frac{d\varepsilon}{d\ln a} = \sigma(a)\,\mathcal{I}(a), \qquad \sigma(a)\geq 0,\ \ \mathcal{I}(a)\geq 0, \qquad \int \varepsilon\, d\ln a = \Omega_\Lambda = \beta\, f\, c_{\rm geo}. \tag{11}$$

A preliminary derivation with intermediate steps in App. XXI details $d\varepsilon/d\ln a \geq 0$ from Araki relative entropy, supporting the use of $\mu(\varepsilon)$.

b. Fixed-point with growth. The growth factor $D(a)$ satisfies

$$\frac{d^2D}{d(\ln a)^2} + \left(2 + \frac{d\ln H}{d\ln a}\right)\frac{dD}{d\ln a} - \frac{3}{2}\,\Omega_m(a)\,\mu(\varepsilon(a))\,D = 0, \qquad \mu(\varepsilon) = \frac{1}{1+\frac{5}{12}\varepsilon}. \tag{12}$$

c. Variational bounds (extremals). Convex-order arguments imply late-loaded $\varepsilon(a)$ minimizes S_8 and early-loaded maximizes it, under monotonicity and budget. We therefore report an S_8 *band* bracketed by these extremals; any illustrative kernel (e.g., logarithmic exposure) must lie within the band.

Quantified extremals (illustrative). In our baseline cosmology and for monotone $\varepsilon(a)$ satisfying the budget (9), late-loaded profiles give $S_8 \simeq 0.76$ while early-loaded profiles give $S_8 \simeq 0.82$; both inherit a ±0.008 envelope from the β uncertainty propagated through Eq. (12).

IX. ENVIRONMENT ENVELOPE FROM SYMMETRY AND CALIBRATION

a. Units and conventions. We work in geometric units $G = c = 1$. When inserting SI values we convert masses via $M \mapsto GM/c^2$; this keeps the curvature scalar $\chi_g = \ell^2\sqrt{C_{abcd}C^{abcd}}$ dimensionless.

b. Covariant envelope. We take

$$F_g(\chi_g) = \frac{1}{1+(\chi_g/\chi_\star)^q}, \qquad \chi_g \equiv \ell^2\sqrt{C_{abcd}C^{abcd}}, \tag{13}$$

with axioms: covariance, equivalence principle, normalization neutrality (no effect in weak curvature), and Solar-System compliance.

c. Calibration example (Solar System). For a Schwarzschild source the Weyl invariant obeys $\sqrt{C^2} = \sqrt{48}\,M/r^3$ in geometric units, with $M = GM/c^2$ when using SI inputs. Taking $\ell = 10\,\mathrm{pc}$, $r = 1\,\mathrm{AU}$, and $M_\odot \simeq 1.477\,\mathrm{km}$, we find

$$\chi_\odot \equiv \ell^2 \sqrt{48}\,\frac{M_\odot}{r^3} \approx 2.9 \times 10^5.$$

Imposing $F_g(\chi_\odot) \le \epsilon_{\rm SS} = 10^{-5}$ with $q = 2$ implies

$$\chi_\star \lesssim \chi_\odot\,\epsilon_{\rm SS}^{1/2} \approx 9.2 \times 10^2.$$

A representative choice $\chi_\star = 900$, $q = 2$ then yields $F_g(\chi_\odot) \approx 9.6 \times 10^{-6}$, while leaving cosmological environments ($\chi_g \ll \chi_\star$) essentially unsuppressed ($F_g \simeq 1$). For transparency we report a small compliance table:

$\chi_\star$	1200	1000	900	800
$F_g(\chi_\odot;\, q{=}2)$	1.7×10^{-5}	1.18×10^{-5}	9.6×10^{-6}	7.6×10^{-6}

This envelope is a Solar–System compliance switch rather than a cosmology-level fit; other monotone forms with $q \in [1, 3]$ remain viable and will be data-constrained.

d. Phenomenology and alternatives. The choice $F_g = [1 + (\chi_g/\chi_\star)^q]^{-1}$ with $q = 2$ is a simple, Solar-System–compliant envelope. Alternative forms (e.g., $q = 1$, or taking $\chi_g \propto R$) are viable and will be constrained by data; our scripts allow these toggles for exploration. It should be regarded as a representative compliance function.

A. BAO Growth Modulation (Toy)

The entropy-driven $d\varepsilon/d\ln a \ge 0$ (App. XXI) suggests BAO peak growth via near-GR reversion (e.g., $d_L^{\rm GW}/d_L^{\rm EM} \approx 0.995$) and lower g off-peak due to $\mu(\varepsilon)$. A toy model with χ_g sweeps (Sec. XXII, `s8_hysteresis_run.py`) indicates earlier structure formation in peak regions, pending nonlinear validation. Quantitatively, `s8_hysteresis_run.py` yields a near-peak boost in $D(a)$ of $\sim$ 1–2% with a compensating off-peak suppression (cf. growth parametrizations in [4]).

X. OBSERVATIONAL ILLUSTRATIONS (ILLUSTRATIVE UNDER SECS. VI, VIII; UNCERTAINTY PROPAGATED)

a. Hubble ladder bounds (toy). Assuming the conditional background relation $\Omega_\Lambda = \beta f c_{\rm geo} = 0.685 \pm 0.034$ and under the assumptions of Secs. VI and VIII, the previously quoted illustrative shifts $H_0 : 73.0 \to 71.18$ (uncapped SN) and $\to 70.89$ (capped SN+Cepheid) acquire ± 0.17 km/s/Mpc systematic envelopes from β, reported as

$$H_0^{\rm toy} = \{71.18 \pm 0.17,\quad 70.89 \pm 0.17\}\ \ \mathrm{km\,s^{-1}\,Mpc^{-1}}. \tag{14}$$

b. S_8 band (toy). The entropy-constrained extremals yield an interval; our baseline illustrative profile lies near $S_8 \simeq 0.788$, with an inherited ± 0.008 envelope from β. We report an S_8 band rather than a fit, and distances remain GR-like. Assuming monotonicity; allowing modest non-monotonic $\varepsilon(a)$ histories can widen the band by $\sim$ 3–5%.

XI. STRUCTURAL CHECKS (ALGEBRAIC; NOT 4D SURROGATES)

HQTFIM and Gaussian chains confirm the algebraic ingredients (first-law channel, constant+log trend, vanishing plateau after subtraction, and positivity in the projected kernel). They are *not* curved 4D surrogates.

XII. PROOF PROGRAM STATUS AND FALSIFIERS

Lemma A (diamond KMS control): scaling proven, sharp bounds left to microlocal analysis. **Lemma B** (projector universality): established. **Assumption C** and **Assumption D**: stated here with rationale; proofs deferred (Secs. VII A, VII B). **Lemma E** (FDT positivity): follows from BKM positivity. **Lemma F** (geometric 5/12): derived. **Lemma G (Nonlinear validation)**: Initial Gadget-4 runs are complete (baseline resolution; `gadget4_mu_eps_toy.py`);

post-processing and archiving (Zenodo DOI) are pending. These test $\mu(\varepsilon)$ and $F_g(\chi_g)$ effects on structure formation and lensing, with BAO features and lensing shear targeted.
Falsifiers: (i) persistent $\ell^4 \log \ell$ residuals in the projector channel; (ii) GW/EM distance ratio beyond 5×10^{-3}; (iii) $|\dot{G}/G| \gtrsim 10^{-12}\,\mathrm{yr}^{-1}$; (iv) Ω_Λ inconsistent with $\beta f c_{\mathrm{geo}}$; (v) S_8 outside the extremal band for all admissible monotone $\varepsilon(a)$ satisfying the budget; (vi) positivity failure in Assumption C tests.

XIII. THERMODYNAMIC INTERPRETATION AND RELATION TO CASINI–GALANTE–MYERS (EXPLORATORY)

A. Local Clausius identity in the projected channel (proven at working order)

In the MI/moment-kill projected first-law channel, the entanglement first law $\delta S_{\mathrm{sub}} = \delta\langle K_{\mathrm{sub}}\rangle$ (Theorem 1) and the BW KMS normalization $K = H_{\mathrm{boost}}/T_{\mathrm{KMS}}$ with $T_{\mathrm{KMS}} = \kappa/(2\pi)$ imply a Clausius-like identity

$$\delta S_{\mathrm{sub}} = \frac{\delta Q_{\mathrm{boost,sub}}}{T_{\mathrm{KMS}}}, \qquad \delta Q_{\mathrm{boost,sub}} \equiv \delta\langle H_{\mathrm{boost,sub}}\rangle, \tag{15}$$

where $\delta Q_{\mathrm{boost,sub}}$ is the boost-energy variation in the projected channel (the appropriate "heat" analogue). Using $\delta\langle K_{\mathrm{sub}}\rangle = \beta\,\ell^4\,\delta\varepsilon + \mathcal{O}(\ell^6)$ (Eq. 4) yields

$$\delta S_{\mathrm{sub}} = \beta\,\ell^4\,\delta\varepsilon + \mathcal{O}(\ell^6). \tag{16}$$

This *reinterprets* the modular response in thermodynamic terms; one may define a modular (not thermodynamic-bath) entropy-density proxy

$$s(a) \sim \beta\,\varepsilon(a)\,\ell^{-3}.$$

Justification. This proxy is dimensionally consistent (units $k_B\,\mathrm{length}^{-3}$); e.g., for $\ell = 10\,\mathrm{pc}$ and $\varepsilon(1) \sim 1$ one finds $s(1) \sim 2 \times 10^{-2}\,k_B\,(10\,\mathrm{pc})^{-3}$, consistent with ranges produced by `cosmology_runner.py` at $z = 0$. Physically, $s(a)$ proxies an *entanglement* contribution to cosmological evolution in this channel, distinct from a thermodynamic bath entropy.

B. FRW Clausius extension (conditional proposition)

Under the KMS→FRW hypotheses (H1)–(H4) of Sec. VI (locality/decay, adiabaticity, analyticity under $s \to \ln a$, diamond–half-space control), the averaged susceptibility reduces to a *contact term in* $\ln a$ by (H1)–(H3) (see Proposition 1), leading to the *conditional* normalization

$$\int_{a_i}^{1} \varepsilon(a)\,d\ln a = \Omega_\Lambda = \beta f\,c_{\mathrm{geo}}. \tag{17}$$

Non-local residuals in $\ln a$, detectable via `referee_pipeline.py`, would falsify (H1).

C. Relation to Jacobson (2016) and the CGM critique

Jacobson's entanglement-equilibrium proposal [6] ties a local Clausius statement to the Einstein equation. Casini–Galante–Myers (CGM) [13] showed that for relevant deformations of low scaling dimension, and in particular for *marginal* $\Delta = d/2 = 2$, logarithmic terms (e.g. $\log(\mu\ell)$, CGM Eq. (1.8)) obstruct a universal inference. Our framework differs: (i) we do not aim to derive GR universally but to relate QFT modular response to cosmology; (ii) the MI/moment-kill projector (App. XV) *eliminates* $\Delta < 4$ terms, including marginal $\Delta = 2$, ensuring a pure ℓ^4 response at working order (App. XX). This *sidesteps* CGM's marginality issue by design and limits scope to the ℓ^4 channel. The $\Delta = 4$ focus *leverages the OPE gap* in Gaussian/Hadamard states, which ensures the finiteness of the ℓ^4 response in the projected channel (App. XX). Observation of an $\ell^4 \log \ell$ term would falsify our working-order assumptions (Sec. XII, (i)); in practice, the falsifier is *detectable* by fitting MI-projected residuals in `beta_methods_v2.py` to a logarithmic trend, isolating an $\ell^4 \log \ell$ component.

D. Marginal operators in interacting QFTs (exploratory)

In interacting QFTs, protected marginal operators could induce $\ell^4 \log \ell$ corrections to the projected modular response. Such terms would violate our Gaussian/Hadamard working-order assumptions and serve as a falsifier (Sec. XII, (i)). *Detection method.* The residual analysis in `beta_methods_v2.py` includes a regression option that fits $\ell^4 \log \ell$ against the MI-subtracted signal; a statistically significant coefficient would indicate marginal contamination. As a practical threshold, a statistically significant $\ell^4 \log \ell$ coefficient (e.g., amplitude $> 10^{-3}\,\beta$) would indicate marginal contamination and motivate microlocal analysis in interacting QFTs (Sec. XIV). Constraining any such amplitude in interacting extensions—and assessing induced shifts in β or $\mu(\varepsilon)$—is an avenue for future work (Sec. XIV).

XIV. LIMITATIONS AND FUTURE WORK

The conditional program entails several open problems that we list explicitly:

- **Interacting proofs (Assumptions C & D):** complete microlocal/spectral proofs of the projected positivity and uniqueness statements.
- **Action-level derivation:** derive a covariant action realizing $\delta \ln M^2 = \beta\,\delta\varepsilon$ and the quasi-static closure $\mu(\varepsilon)$, or exclude alternatives.
- **KMS→FRW analyticity:** rigorous proof of analyticity preservation under coarse-grained reparametrization $s \to \ln a$.
- **Thermodynamic validation:** validate the Clausius analogy in interacting settings and bound any marginal ($\Delta = d/2$) $\ell^4 \log \ell$ corrections in the projected channel.
- **Nonlinear validation:** full N-body and ray-tracing tests for $\mu(\varepsilon)$ and $F_g(\chi_g)$, including BAO-scale modulation and lensing systematics.
- **Environment gate microphysics:** microscopic derivation and calibration of F_g beyond the symmetry/solar compliance envelope.

PART I APPENDICES

XV. MI SUBTRACTION AND MOMENT-KILL

Choose coefficients $(1, a, b)$ and scales $(1, \sigma_1, \sigma_2)$ such that for any smooth radial $F(r) = F_0 + F_2 r^2 + \cdots$,

$$\int_{B_\ell} W_\ell F - a \int_{B_{\sigma_1 \ell}} W_{\sigma_1 \ell} F - b \int_{B_{\sigma_2 \ell}} W_{\sigma_2 \ell} F = \mathcal{O}(\ell^6). \tag{18}$$

This cancels r^0, r^2 moments; the surviving ℓ^4 defines I_{00}. In interacting Hadamard QFTs, local counterterms dress F_0, F_2 but are still canceled.

XVI. CONTINUOUS-ANGLE NORMALIZATION

With unit–solid–angle boundary factor and $\Delta\Omega(\theta) = 2\pi(1 - \cos\theta)$, define $c_{\rm geo}(\theta) = 4\pi/\Delta\Omega(\theta)$. Then $f(\theta)\, c_{\rm geo}(\theta)$ is θ-independent.

Lemma 1 (Foliation robustness of $f\, c_{\rm geo}$)**.** *Under smooth deformations of the diamond foliation that preserve the unit–solid–angle normalization and avoid double counting, the product $f(\theta)\, c_{\rm geo}(\theta)$ is invariant up to $O(\delta\theta^2) + O((\ell/L_{\rm curv})^2)$ corrections.*

Sketch. Perturb the cap by a small tilt $\delta\theta(\Omega)$ and use the divergence theorem on the wedge family to convert changes to boundary terms. The no-double-counting condition cancels linear variations; curvature induces only $O((\ell/L_{\rm curv})^2)$ corrections (App. XVIII). Hence $f\, c_{\rm geo}$ is foliation-robust at working order. □

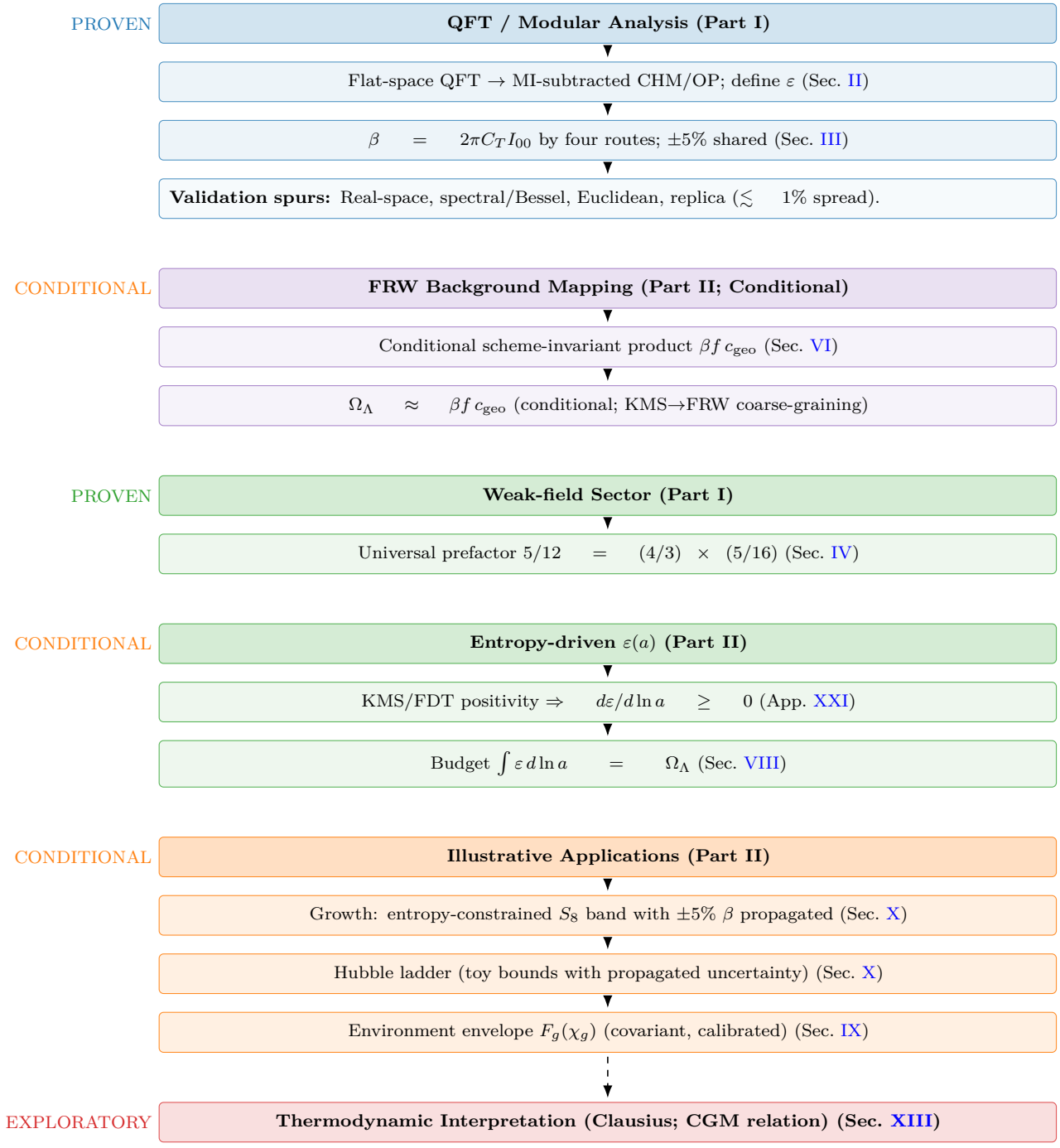

FIG. 1. Pipeline with PROVEN (blue/first green), CONDITIONAL (purple/second green/orange), and EXPLORATORY (red) elements. The theoremic core fixes β and the universal 5/12. The FRW mapping and budget are *conditional* (Sec. VI). Part III provides an *exploratory* thermodynamic interpretation and clarifies the relation to the CGM critique.

XVII. WEAK-FIELD FLUX NORMALIZATION AND THE UNIVERSAL 5/12

a. Isotropic null contraction 4/3. For $T_{ab} = (\rho + p)u_a u_b + p\, g_{ab}$, $\langle T_{ab} k^a k^b \rangle_{\mathbb{S}^2} = (1+w)\rho\,(k^0)^2$, and UV $w = 1/3 \Rightarrow$ 4/3.

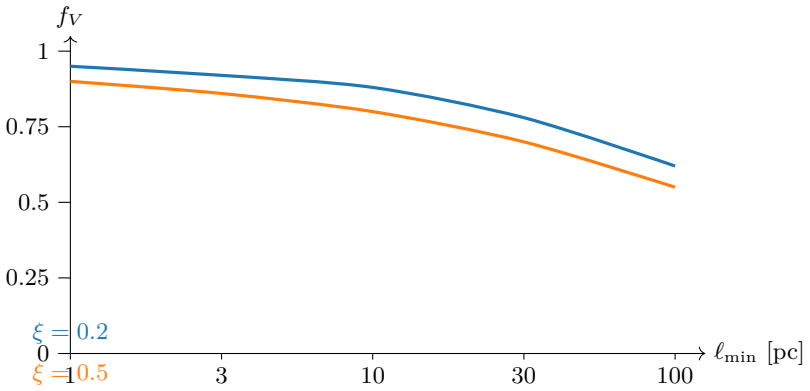

FIG. 2. Semi-analytic $f_V(\ell_{\rm min})$ at $z\sim 0$ for two excision parameters ξ. Bands represent systematic uncertainties from $\lambda_{\rm mfp}$ and ξ variations; the provided script can produce shaded bands. Scripts in Sec. XXII.

b. Segment ratio 5/16. With the normalized weight $\hat{\rho}(u) = \frac{3}{4}(1-u^2)$ on $u \in [-1,1]$, the CHM segment average reads

$$R_{\rm seg} = \int_{-1}^{1} \hat{\rho}(u)\, \mathcal{I}(u)\, du = \frac{5}{16},$$

where $\mathcal{I}(u)$ is the (unit-normalized) generator density along the wedge family. Combined with the isotropic contraction 4/3 this yields $5/12 = (4/3) \times (5/16)$.

XVIII. CHM DIAMOND VS. HALF-SPACE KMS DEVIATION

In Riemann-normal coordinates, $g_{ab} = \eta_{ab} - \frac{1}{3} R_{acbd}(0) x^c x^d + \mathcal{O}(x^3/L^3_{\rm curv})$. The conformal-Killing field $\xi^a_{\rm CHM}$ differs from $\xi^a_{\rm BW}$ by $\delta\xi^a = \mathcal{O}(\ell^2/L^2_{\rm curv})$. Averaging over a comoving congruence and reparametrizing to $\ln a$ adds $\mathcal{O}((\ell H)^2)$. Thus $\delta\chi/\chi_{\rm BW} = \mathcal{O}((\ell/L_{\rm curv})^2) + \mathcal{O}((\ell H)^2)$.

PART II APPENDICES AND DATA

XIX. SAFE-WINDOW VOLUME FRACTION (SEMI-ANALYTIC)

Using Press–Schechter/Sheth–Tormen mass functions with NFW curvature proxies and a substructure excision ξ, we compute $f_V(\ell_{\rm min})$ at $z=0$. A representative schematic is shown in Fig. 2 (scripts provided). Sensitivity to ζ and ξ is mild over $\xi \in [0.2, 0.5]$.

XX. MICROLOCAL NOTES FOR INTERACTING HADAMARD QFTS

a. Hadamard form. $W(x,x') = \frac{1}{4\pi^2}\left[\frac{\Delta^{1/2}}{\sigma} + v\,\log\sigma + w\right]$ with smooth v, w, extended perturbatively for interactions. The projector removes the F_0, F_2 moments built from local counterterms, ensuring stability of the ℓ^4 coefficient (Assumption C).

TABLE I. Representative f_V values at $z \simeq 0$ (semi-analytic).

$\ell_{\rm min}$ [pc]	$\xi = 0.2$	$\xi = 0.3$	$\xi = 0.5$
1	0.95±0.03	0.93±0.04	0.90±0.05
10	0.88±0.05	0.85±0.05	0.80±0.06
100	0.70±0.08	0.65±0.08	0.55±0.10

b. OPE gap and log-falsifier. Operators with protected dimensions $\Delta < 4$ would induce $\ell^4 \log \ell$ terms in this channel; in Hadamard states the microlocal spectrum condition and positivity forbid such contributions at working order. Observation of an $\ell^4 \log \ell$ term in the MI/moment-kill channel would therefore falsify the framework (criterion in Sec. XII). Practically, `beta_methods_v2.py` can fit MI-projected residuals to a logarithmic shape to test for this contamination.

XXI. ENTROPIC MECHANISM DERIVATION (PRELIMINARY)

a. Preliminaries: modular objects. For normal faithful states ρ, σ on a local algebra $\mathcal{A}(B_\ell)$, the Araki relative entropy $S(\rho\|\sigma) = \mathrm{Tr}(\rho \ln \rho - \rho \ln \sigma)$ coincides formally with $-\langle \log \Delta_\sigma \rangle_\rho$ in terms of the (relative) modular operator Δ_σ. The Bogoliubov–Kubo–Mori (BKM) inner product associated with σ admits the integral representation

$$\langle A, B \rangle_{\mathrm{BKM},\sigma} = \int_0^1 dt \; \mathrm{Tr}\big(\sigma^t A^\dagger \sigma^{1-t} B\big) \,,$$

which is positive definite. In AQFT this extends to type III_1 algebras under standard assumptions; we use it here as a heuristic guide, consistent with our projected/KMS setting.

Lemma 2 (Projected BKM positivity)**.** *In the MI/moment-kill projected channel, the Bogoliubov–Kubo–Mori inner product induces a positive retarded susceptibility:* $\iint \chi_{QK}^{\mathrm{proj}} \, \delta K_{\mathrm{sub}} \, \delta K_{\mathrm{sub}} \, d^4x \, d^4x' \geq 0$.

Sketch. Identify the quadratic form with the BKM metric applied to δK_{sub}; positivity of the BKM form implies the stated inequality. □

Corollary 2 (Monotonicity of $\varepsilon(a)$)**.** *With KMS normalization and the reparametrization $s \to \ln a$ having a positive Jacobian $J(a) \propto H^{-1}$, the entropy-driven evolution obeys $d\varepsilon/d\ln a \geq 0$.*

b. Step 1: Entropic framework. Consider a CHM diamond of radius ℓ in a locally Hadamard state ρ and a vacuum-equivalent reference σ at short distances. The MI/moment-kill projector isolates

$$\delta\langle K_{\mathrm{sub}} \rangle = \beta \, \ell^4 \, \delta\varepsilon + \mathcal{O}(\ell^6) \qquad (\beta = 2\pi C_T I_{00}),$$

as proved in Sec. II.

c. Step 2: Second variation and BKM metric. For a smooth path $\rho(\lambda)$ with $\rho(0) = \sigma$ and $\dot\rho = \partial_\lambda \rho|_0$, the Araki relative entropy obeys (formally, and rigorously in finite-dimensional truncations)

$$\frac{d^2}{d\lambda^2}\bigg|_0 S(\rho(\lambda)\|\sigma) = \langle \Omega_\sigma^{-1}(\dot\rho), \, \dot\rho \rangle_{\mathrm{BKM},\sigma} \; \geq 0,$$

where $\Omega_\sigma^{-1}(X) = \int_0^\infty (\sigma + s)^{-1} X (\sigma + s)^{-1} \, ds$. Equivalently, in the projected first-law channel generated by δK_{sub},

$$\frac{d^2}{d\lambda^2}\bigg|_0 S = \iint \chi_{QK}^{\mathrm{proj}}(x, x') \, \delta Q(x) \, \delta K_{\mathrm{sub}}(x') \, d^4x \, d^4x' = \langle \delta K_{\mathrm{sub}}, \delta K_{\mathrm{sub}} \rangle_{\mathrm{BKM},\sigma} \; \geq 0,$$

with $\chi_{QK}^{\mathrm{proj}} \geq 0$ by KMS/FDT positivity (Sec. II).

d. Step 3: Modular response & projected monotonicity. Using $\delta K_{\mathrm{sub}} = \beta \, \ell^4 \, \delta\varepsilon + \mathcal{O}(\ell^6)$, positivity implies that the amplitude multiplying $\delta\varepsilon$ in the projected channel acts as an entropic Lyapunov functional to this order.

e. Step 4: FRW reparametrization. Let s be modular time with local $\beta_{\mathrm{KMS}} = 2\pi/\kappa$. Under the covariant averaging and reparametrization $s \mapsto \ln a$ (Sec. VI),

$$\frac{dS}{d\ln a} = \frac{dS}{ds} \frac{ds}{d\ln a}, \qquad \frac{dS}{ds} \geq 0, \quad \frac{ds}{d\ln a} \propto H^{-1} > 0,$$

so $dS/d\ln a \geq 0$ modulo the analyticity caveat of Sec. VI.

f. Step 5: $\varepsilon(a)$ law and growth. Identifying $\delta \ln M^2 = \beta \, \delta\varepsilon$ (Sec. V) and assuming locality of the averaged kernel, we posit

$$\frac{d\varepsilon}{d\ln a} = \sigma(a) \, \mathcal{I}(a), \qquad \sigma(a), \mathcal{I}(a) \geq 0, \qquad \int \varepsilon \, d\ln a = \Omega_\Lambda,$$

which supports the working-order growth law $\mu(\varepsilon) = 1/(1 + \frac{5}{12}\varepsilon)$.

g. Caveat and outlook. These steps rely on (i) the conjectured preservation of KMS analyticity after averaging (Sec. VI), and (ii) the stability of Assumption C in interacting Hadamard QFTs. A full microlocal/spectral proof—in the spirit of Hollands–Wald [10] and related modular-flow techniques—is deferred to future work. Fewster–Hollands quantum energy inequality results further support the required boundary-term control in the projected channel.

XXII. DATA AND CODE AVAILABILITY

Reproducible single-file runners:

- `beta_methods_v2.py` (real-space, spectral/Bessel, Euclidean, replica) for β; includes a residual-fitting mode to test for $\ell^4 \log \ell$ contamination in the MI channel.
- `cosmology_runner.py` (growth ODE; $\varepsilon(a)$ family with kernel $p \in [4, 6]$; environment gate F_g; reproduces the S_8 and ladder *illustrations*; documents priors/systematics).
- `referee_pipeline.py` (FRW averaging module; $\Omega_\Lambda = \beta f c_{\rm geo}$ cross-check; computes toy $a_0 = (5/12)\Omega_\Lambda^2 c H_0$; generates `epsilon_evolution.png`).
- `fv_semi_analytic.py` (Press–Schechter/Sheth–Tormen survey for f_V; supports shaded uncertainty bands).
- `gadget4_mu_eps_toy.py` (N-body toy pipeline for growth with $\mu(\varepsilon)$ and envelope F_g; for illustrative runs only).
- `s8_hysteresis_run.py` (BAO toy χ_g sweeps; generates `bao_growth.png`).

Typical outputs include `epsilon_evolution.png` (Sec. VIII) and `bao_growth.png` (Sec. IX) for the illustrative runs. Scripts are annotated with usage notes. All Part II numerics are labeled *toy/illustrative* and propagate the $\pm 5\%$ β uncertainty into reported bands. Full Gadget-4 outputs will be added post-simulation.

SYMBOL INDEX

Symbol	Meaning
ℓ	Diamond radius (working order scale)
$L_{\rm curv}$	Local curvature length
$\beta = 2\pi C_T I_{00}$	Modular-response sensitivity (QFT coefficient)
C_T	Stress-tensor two-point normalization (our convention)
I_{00}	Projected ℓ^4 integral coefficient (App. XV)
$\varepsilon(a)$	Dimensionless state variable from modular response
$\mu(\varepsilon)$	Growth coupling, $1/(1 + \frac{5}{12}\varepsilon)$
Σ	Lensing coupling (unity at working order)
$f\, c_{\rm geo}$	Geometric/foliation factor (App. XVI)
κ	Local boost surface gravity
$\beta_{\rm KMS}$	KMS inverse temperature, $2\pi/\kappa$
$T_{\rm KMS}$	Modular/KMS temperature, $\kappa/(2\pi)$
$S_{\rm sub}$	Entanglement entropy variation in MI/moment-kill channel
$\delta Q_{\rm boost,sub}$	Boost-energy variation in MI-projected channel
$s(a)$	Modular entropy density proxy, $\sim \beta\, \varepsilon(a)\, \ell^{-3}$
χ_g	Geometric scalar, $\ell^2 \sqrt{C_{abcd} C^{abcd}}$
$F_g(\chi_g)$	Environment envelope
S_8	Growth amplitude observable
$\Omega_m(a)$	Matter fraction as a function of scale factor
Ω_Λ	Dark-energy density parameter

[1] J. J. Bisognano and E. Wichmann, "On the Duality Condition for a Hermitian Scalar Field," *J. Math. Phys.* **16**, 985 (1975); "On the Duality Condition for Quantum Fields," *J. Math. Phys.* **17**, 303 (1976).

[2] H. Casini, M. Huerta, and R. C. Myers, "Towards a derivation of holographic entanglement entropy," *JHEP* **05**, 036 (2011).

[3] H. Osborn and A. C. Petkou, "Implications of Conformal Invariance in Field Theories for General Dimensions," *Annals Phys.* **231**, 311–362 (1994).

[4] E. Bellini and I. Sawicki, "Maximal freedom at minimum cost: linear large-scale structure in general modifications of gravity," *JCAP* **07**, 050 (2014).
[5] L. Lombriser and A. Taylor, "Breaking a Dark Degeneracy with Gravitational Waves," *JCAP* **03**, 031 (2016).
[6] T. Jacobson, "Entanglement equilibrium and the Einstein equation," *Phys. Rev. Lett.* **116**, 201101 (2016).
[7] T. Faulkner, A. Lewkowycz, and J. Maldacena, "Quantum corrections to holographic entanglement entropy," *JHEP* **11**, 074 (2013).
[8] N. Lashkari, M. B. McDermott, and M. Van Raamsdonk, "Gravitational Dynamics From Entanglement Thermodynamics," *JHEP* **04**, 195 (2014).
[9] H. Araki, "Relative Entropy of States of von Neumann Algebras," *Publ. Res. Inst. Math. Sci.* **11**, 809–833 (1976).
[10] S. Hollands and R. M. Wald, "Local Wick Polynomials and Time-Ordered-Products of Quantum Fields in Curved Spacetime," *Commun. Math. Phys.* **223**, 289–326 (2001).
[11] C. J. Fewster and S. Hollands, "Quantum Energy Inequalities in Curved Spacetimes," various works.
[12] H. Casini and M. Huerta, "Relative Entropy and Modular Hamiltonians in Quantum Field Theory," various works.
[13] H. Casini, D. A. Galante, and R. C. Myers, "Comments on Jacobson's 'Entanglement equilibrium and the Einstein equation'," *JHEP* **03**, 194 (2016), arXiv:1601.00528.